Silicon carbide-based functional components in the Visible Emission Line Coronagraph on-board the ADITYA-L1 mission

Bhaskar Prasad Saha[1], Dulal Chandra Jana[1,*], Prasenjit Barick[1], V. Natarajan[2], Suresh Venkata[2], Abhijit A. Adoni[3], D. R. Veeresha[3], R. Venkateswaran[4], P. U. Kamath[2], Roy Johnson[1], K. V. Sriram[4], B. Raghavendra Prasad[2] and G. Padmanabham[1]

[1]International Advanced Research Centre for Powder Metallurgy and New Materials, Balapur Post, RCI Road, Hyderabad 500 005, India
[2]Indian Institute of Astrophysics, 2nd Block, Koramangala, Bengaluru 560 034, India
[3]U. R. Rao Satellite Centre, Old Airport Road, Vimanapura Post, Bengaluru 560 017, India
[4]Laboratory for Electro-Optics Systems, First Phase, Peenya Industrial Estate, Bengaluru 560 058, India

A state-of-the-art Visible Emission Line Coronagraph (VELC) payload on-board India's solar mission ADITYA-L1 was designed to study various solar phenomena. To maintain the thermal stability of the system, VELC design recommends silicon carbide (SiC)-based components because of their outstanding mechanical, thermal and optical properties. In particular, a SiC-based tertiary mirror (M3) was used for the collection of undesired sunrays and reflecting them out from the system, and a SiC radiator plate (popularly known as a cold finger) for efficient heat dissipation from the mirror and, in turn, from the system. This article describes the processing and evaluation of SiC-based M3 mirror and cold finger for VELC. The substrates for M3 mirror and cold finger were processed through dry pressing of SiC powder with the required formulation, followed by machining and temperature-assisted densification under an inert atmosphere. SiC components developed using powder metallurgical technique exhibited about 98.4% relative density (RD) and achieved the structural and thermal requirements of M3 mirror and cold finger. The optical requirement of M3 mirror was achieved through a coating of SiC substrate with 100% RD employing chemical vapour deposition followed by surface grinding and polishing. The final mirror achieved a surface flatness better than 20 nm, and microroughness data showed less than 5.1 Å root mean square surface roughness in a spatial scale of 0.02 to 0.9 mm.

Keywords: Chemical vapour deposition, coronagraph, relative density, silicon carbide, solar mission.

THE study of the sun's corona has been of immense scientific interest over centuries to understand numerous solar phenomena, including investigation of coronal and coronal-loop plasma, solar corona heating mechanisms, the origin of coronal magnetic fields and how they drive plasma heating, solar storms, flares and coronal mass ejection (CME), dynamics of large-scale transients, controlling factors for space weather, etc.[1,2]. The data obtained through imaging and spectroscopic techniques during solar eclipses and coronagraphs are the most direct and reliable basis for understanding the above phenomena. The Visible Emission Line Coronagraph (VELC) payload on-board India's first space solar mission ADITYA-L1 has been designed for simultaneous imaging, spectroscopic and spectro-polarimetric observations of the inner solar corona[3]. The solar corona imaging provides information about the coronal intensity and its variation with time and space. At the same time, spectroscopy data are useful in analysing the velocity and spectral line-width variation. Therefore, spectroscopic information is essential for a better understanding of the physical and dynamic behaviour of the solar corona and its heating mechanisms. Further, the polarimetric capabilities of VELC will help study the drivers for space weather and its prediction.

One of the primary aims of the solar mission is to study the solar corona between $1.05R_0$ and $3R_0$ (R_0 is the solar radius) by analysing imaging and spectroscopic data from VELC[1,4]. The VELC assembly has an off-axis concave parabolic primary mirror (M1) of about 200 mm diameter that receives sunlight directly and then reflects it to another spherical mirror (M2). M2 acts as an internal occulter, which reflects the coronal light but allows the disc light to pass through a hole in its centre. Then, the coronal light is sent through a dichroic beam splitter (DBS) to separate it into imaging and spectroscopy channels. Meanwhile, the undesirable disc light passing through the central hole of M2 is further directed to a tertiary mirror (M3) and then reflected out of the instrument. The detailed optical layout of VELC is described elsewhere[3].

The sun's heat load on M1 mirror is about 25 W, and 95% of this heat is received on the surface of mirror M3,

*For correspondence. (e-mail: janad@arci.res.in)

with a diameter of about 40 mm. Therefore, M3 should be stable at such a high heat load to minimize the scattering issues. Also, the high heat load on M3 may increase its temperature to more than 100°C compared to the required operating temperature within a limit of 22° ± 3°C. The temperature of M3 can be controlled through a heat dissipation mechanism by connecting a radiator plate (also known as a cold finger) of high thermal conductivity material. The heat from the front surface of the mirror passes into the cold finger passively due to the temperature difference between the source (M3 mirror) and the sink (radiator plate). Figure 1 shows the schematic assembly of M3 and cold finger.

Silicon carbide (SiC) was chosen as the material for M3 and cold finger to meet the above requirements because of its excellent properties, including superior thermal conductivity and a lower coefficient of thermal expansion (CTE), along with its temperature stability (high melting point, stable phase and chemical inertness), as well as homogenous and isotropic behaviour[5]. Also, the high stiffness and mechanical properties of SiC help retain the mirror's geometrical integrity. Further, fully dense SiC can be polished to an extremely smooth surface, root mean square (RMS), surface roughness of polished surface can be as low as <1 nm, to minimize scattering from the surface of the mirror. Although M3 and cold finger are based on SiC, the type of material and processing technique are different for these components. The cold finger is a monolithic hexagonal (α) SiC that exhibits about 98.4% relative density (RD). In comparison, M3 comprises an α-SiC substrate (RD ~98.4%) that satisfies the structural requirements of the mirror and 100% RD β (cubic)-SiC coating to achieve the optical properties[5]. The present article provides an overview of the fabrication of SiC-based cold finger and M3, followed by an evaluation of critical properties to meet the operational requirements.

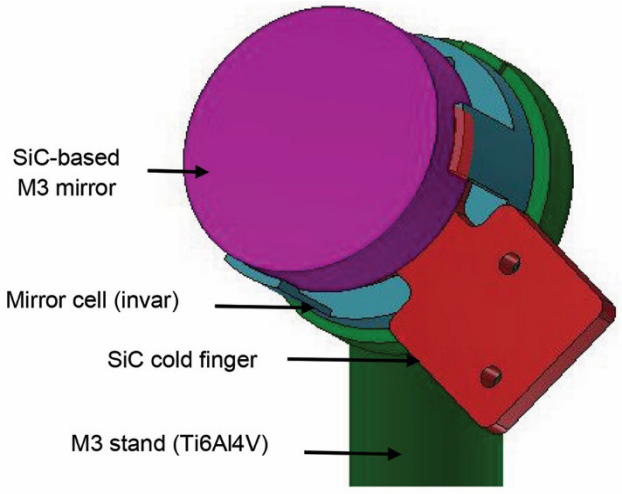

Figure 1. Schematic diagram of SiC-based M3 mirror and cold finger assembly in Visible Emission Line Coronograph.

Processing of SiC components

The substrate for M3 and cold finger was fabricated through consolidation of SiC powder employing the powder metallurgy technique. The process involved compaction of SiC powder through uniaxial pressing followed by low-temperature heat treatment. Subsequently, the parts were machined and then sintered at an elevated temperature in the presence of sintering additives under an inert atmosphere. The process can produce high-quality sintered SiC (S-SiC) components that meet the operational requirements from structural and thermal viewpoints. However, S-SiC components processed through powder metallurgy have limitations for use as the reflecting surface of a mirror due to the non-uniform microstructure and the presence of residual pores. Hence, the monolithic S-SiC processed by powder consolidation technique can be directly used for cold finger applications. Meanwhile, for mirror applications, the S-SiC substrate was further coated with a dense SiC through chemical vapour deposition (CVD). Finally, the CVD-SiC coated surface was polished to obtain the reflecting surface of the mirror. Figure 2 shows the steps in fabricating the SiC cold finger and mirror. Figure 3 shows photographs of the processed SiC components, and the various aspects of their fabrication are discussed subsequently.

S-SiC components through powder consolidation

Commercial-grade, spray-dried α-SiC granules (Densitec 15, Saint-Gobain Ceramic Materials, Norway) were used as the starting material. The spherical-shaped SiC granules (size: 10–80 μm) comprise primary particles with an average size of about 1 μm. The formulation contains approximately 3.0 wt% carbon in the form of phenolic resin (thermosetting type) and 1 wt% B_4C as sintering additives. While the spherical-shaped SiC granules with better flowability (w.r.t. primary particles) help reduce density variation in the compacted parts, phenolic resin improves green strength for easy handling and green machining. Further, carbon residue from resin decomposition was one of the additives for sintering SiC. Boron was another additive in the powder formulation as B_4C.

The first step of powder consolidation involved compaction of SiC granules into the circular disc by uniaxial pressing. Then, the parts were heat-treated at about 500°C in an inert atmosphere to remove organic binders. Usually, binder removal is incomplete in this temperature regime, but the increase in strength due to the network formation of partially decomposed resin helps in the green machining of SiC components. After binder removal, circular shape SiC compacts were machined to the pre-designed shapes of cold finger and mirror substrate. SiC machining before sintering is desirable because of the high hardness of SiC (after diamond and BN), which is often manifested in longer machining times and requires expensive diamond tools.

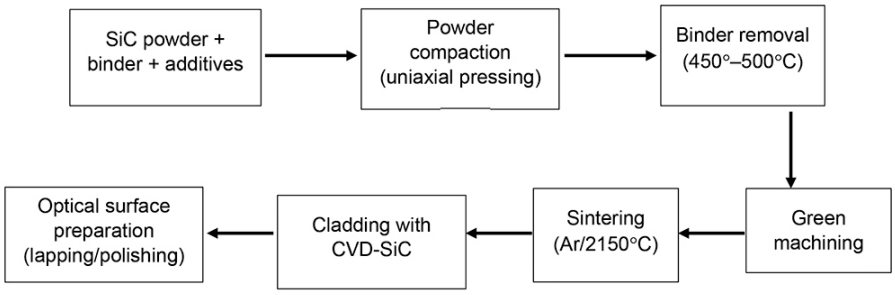

Figure 2. Flow-sheet diagram for processing SiC-based cold finger and mirror (M3). While the processing of cold finger involves steps up to sintering, M3 processing follows the subsequent steps (CVD-SiC coating and lapping/polishing).

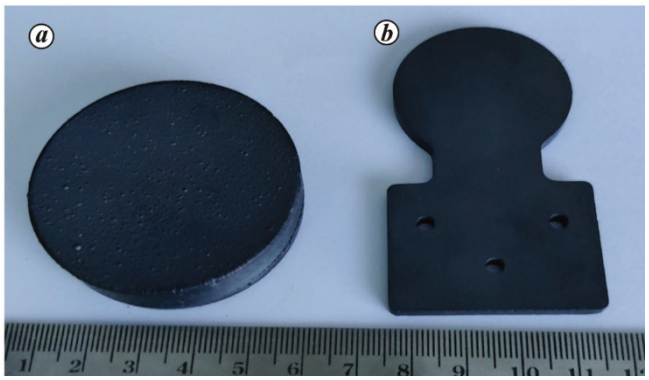

Figure 3. Photographs of processed SiC components: (***a***) 40 mm dia CVD-coated mirror blank, and (***b***) cold finger (overall size: 72.5 × 20.0 × 3.5 mm^3).

The machined parts were densified at 2150°C under an inert atmosphere with a constant flow of argon. The rate of heating and cooling was controlled to avoid thermally induced cracks and warpages in the sintered components. These undergo shrinkage (~20%) during densification due to the formation of interparticle bonding through thermally activated mass transport processes and porosity removal. Hence, the sintering of SiC resulted in an increase in density (up to 98.4% RD). The densification of SiC was enhanced with the help of carbon and boron, which were in powder form as phenolic resin and B_4C respectively. Although the exact role of carbon and boron from additives for sintering of covalently bonded SiC is yet to be known completely, various densification mechanisms have been reported, including grain boundary or lattice diffusion, transient liquid phase sintering, etc.[6]. Finally, the dimensional accuracy of S-SiC components achieved by surface grinding technique.

Chemical vapour deposition

The reflecting surface of S-SiC substrate was cladded with a dense layer of CVD-grown SiC. Methyltrichlorosilane (CH_3SiCl_3, MTS) was used as the precursor for the deposition of CVD-SiC clad layer. The chemical reaction for MTS decomposition to SiC at 1400°C in the presence of H_2 is given below.

$$CH_3SiCl_3 \rightarrow SiC + 3HCl. \quad (1)$$

The concentration and growth rate of the reactants were controlled using argon as the diluent. The CVD-SiC clad layer formed at a much lower temperature than the sintering of SiC and was free from impurities and sintering additives. Therefore, CVD-SiC is a single-phase material that exhibits a homogenous microstructure. Full density (100% RD) can be achieved in CVD-grown SiC through judicious control of various process parameters, including temperature, partial pressure of the reactants and their stoichiometry, and gas flow dynamics. Decomposition kinetics of MTS and optimization of process parameters to achieve theoretical density (100% RD) in CVD-SiC are reported in the literature[7].

Properties of S-SiC and CVD-SiC

The SiC specimens processed along with the SiC components were characterized in terms of their density, crystal structure and other properties. Table 1 shows a comparison of the properties of S-SiC and CVD-SiC. As shown in the table, S-SiC formed through powder metallurgy route exhibits a maximum density 3.16 g cm^{-3} (98.4% RD) compared to that of 3.21 g cm^{-3} (100% RD) achieved in CVD-SiC under a set of optimized CVD parameters, including temperature, pressure, reactants stoichiometry, reactants flow dynamics, etc.[5]. The higher density in CVD-SiC compared to S-SiC is manifested in other properties such as Vickers' hardness, Young's modulus and thermal conductivity (Table 1). Figure 4 *a* and *b* shows SEM photomicrographs on the polished surface of S-SiC and CVD-SiC respectively. Figure 4 *a* shows the presence of residual pores and inclusions on the polished surface, while Figure 4 *b* shows that the surface is free from any defects. Therefore, CVD-SiC can be polished to an extremely low roughness surface compared to S-SiC.

Table 1. Properties of S-SiC and CVD-SiC

Properties	S-SiC	CVD-SiC
Density (g cm^{-3})	3.16 (98.4 % RD*)	3.21 (100% RD)
Phase	α (hexagonal) SiC (6H and 4H polytypes)	α (cubic) SiC (3C polytype)
Vickers hardness, $HV_{500\ g}$** (GPa)	25.3	26.1
Young's modulus (GPa)	415	457
Coefficient of thermal expansion (CTE × 10^{-6} K^{-1})	2.52 (from –125°C to room temperature (RT)) 4.49 (from RT to 1000°C)	2.57 (from –125° to 40°C)[8]
Thermal conductivity (W m^{-1} K^{-1})	143	193 (ref. 8)

*RD indicates relative density. **HV measured at 500 g indentation load.

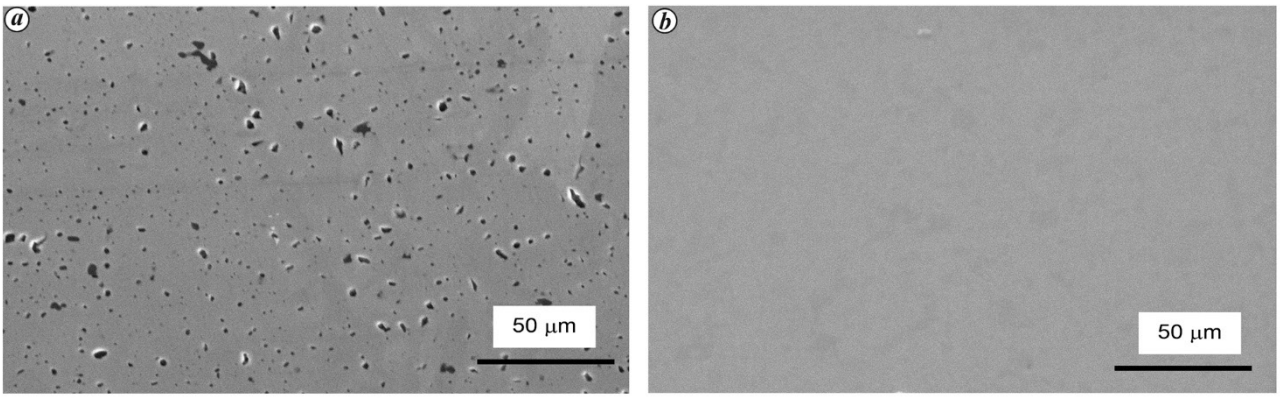

Figure 4. Polished surface SEM photomicrographs of (***a***) S-SiC and (***b***) CVD-SiC.

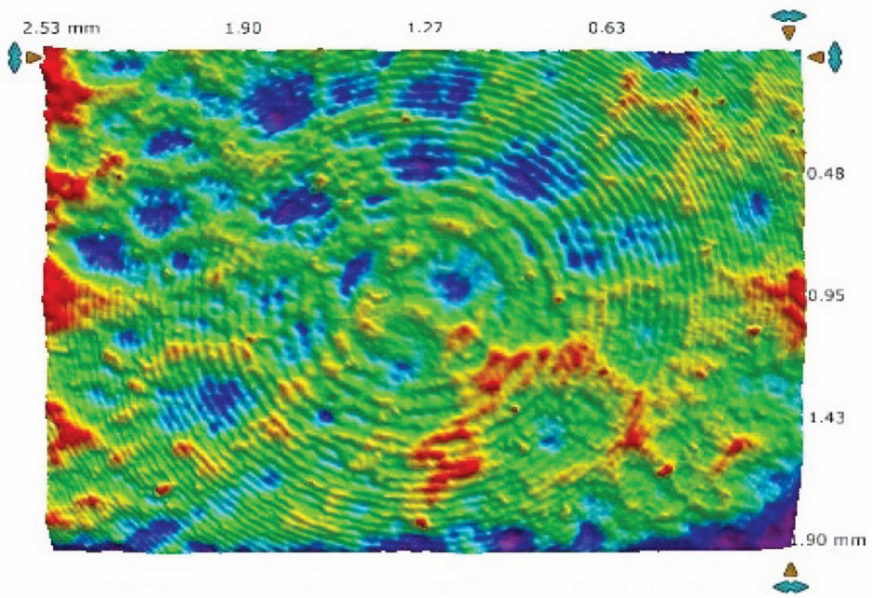

Figure 5. Surface roughness map on polished surface of mirror M3 using a 3D optical profilometer (Bruker, USA). RMS surface roughness (R_q) = 5.1 Å (with a spatial scale of 0.02 to 0.9 mm, field of view 1.90 mm × 2.53 mm and 2.5× magnification).

Preparation of optical surface

The CVD-SiC clad layer on M3 was processed further to generate the optical surface in a sequential manner. Initially, the CVD-coated SiC mirror blank was subjected to surface grinding to remove the non-uniform coating. Then, a concave profile on SiC blank was generated through lapping with the help of a full tool (composite tool of negative profile) and coarse grit (45–15 μm) diamond paste. Finally, the reflecting surface was generated by diamond paste

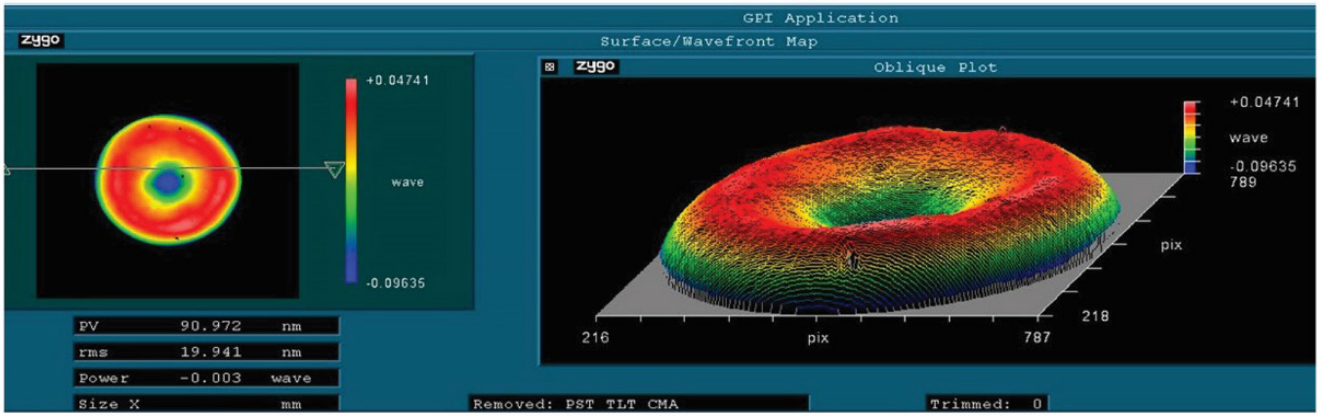

Figure 6. Surface figure measurement data on mirror M3 using an optical interferometer (Zygo, USA).

polishing CVD-SiC with a gradual decrease of grit size from 9 to less than 1 μm. Figure 5 shows the surface roughness map on the polished mirror M3 evaluated using a three-dimensional optical Bruker profilometer. As the figure shows, M3 exhibits about 5.1 Å RMS surface roughness (R_q) in the spatial scale of 0.02–0.9 mm and field of view 1.90 mm × 2.53 mm. Figure 6 shows the measurement of the surface figure using a non-contact optical interferometer (Zygo, USA). A surface figure better than 20 nm was achieved in the finished mirror.

Conclusion

The SiC-based mirror substrate and cold finger for VELC payload on-board ADITYA-L1 were processed through the dry pressing of binder and additives containing SiC powder, followed by machining and pressureless sintering under an inert atmosphere. S-SiC exhibited about 98.4% RD and achieved the mechanical and thermal requirements of the mirror substrate and cold finger. M3 substrate was coated with 100% RD CVD-SiC, and then the optical surface was generated on CVD-SiC upon grinding and polishing. The surface roughness map with the help of a 3D optical profilometer on the polished mirror showed less than 5.1 Å RMS surface roughness and better than 20 nm surface figure.

1. Prasad, B. R. *et al*., Visible emission line coronagraph on Aditya-L1. *Curr. Sci.*, 2017, **113**(4), 613–615.
2. Green, L. M., Török, T., Vršnak, B., Manchester, W. and Veronig, A., The origin, early evolution and predictability of solar eruptions. *Space Sci. Rev.*, 2018, **214**(46), 1–52; doi:10.48550/arXiv.1801.04608.
3. Raj Kumar, N., Singh, J., Prasad, R. B. and Suresh, N. V., Optical design of visible emission line coronagraph on Indian space solar mission Aditya-L1. *Exp. Astron*., 2018; https://doi.org/10.1007/s10686-017-9569-7.
4. Singh, J., Prasad, B. R., Venkata, S. and Kumar, A., Exploring the outer emission corona spectroscopically by using Visible Emission Line Coronagraph (VELC) onboard ADITYA-L1 mission. *Adv. Space Res*., 2019, **64**, 1455–1464.
5. Jana, D. C. and Saha, B. P., Silicon carbide-based lightweight mirror blanks for space optics applications. In *Handbook of Advanced Ceramics and Composites* (eds Mahajan, Y. and Johnson, R.), Springer Nature, Switzerland AG, 2020, pp. 1135–1163.
6. Jana, D. C., Sundararajan, G. and Chattopadhyay, K., Effective activation energy for the solid-state sintering of silicon carbide ceramics. *Metall. Mater. Trans. A*, 2018, **49**, 5599–5606.
7. Schlichting, J., Chemical vapor deposition of silicon carbide. *Powder Metell. Int*., 1980, **12**, 196–200.
8. Goela, J. S., Pickering, M. A., Taylor, R. L., Murry, B. W. and Lompado, A., Properties of chemical-vapour-deposited silicon carbide for optics applications in severe environments. *Appl. Opt.*, 1991, **30**, 3166–3175.

Received 11 January 2021; accepted 18 September 2023

doi: 10.18520/cs/v125/i12/1323-1327